TURKISH ENERGY, NUCLEAR AND MINERAL RESEARCH AGENCY
TURKISH JOURNAL OF NUCLEAR SCIENCES
E-ISSN: 2791-7185
https://dergipark.org.tr/tr/pub/tjns

Antimicrobial Photodynamic Therapy Using Indocyanine Green Loaded FDG Conjugated Cubic Iron Oxide (C-Fe_3O_4) Nanoparticles

Önder Bakır [1,*], Kadriye Büşra Karatay [1], Elif Tutun [1], Volkan Yasakçı [1], Gillian Pearce [2], Perihan Unak [1]

[1] Ege University, Institute of Nuclear Sciences, Department of Nuclear Applications, 35100 Bornova, Izmir, Türkiye
[1] Aston University, School of Engineering and Applied Sciences, Birmingham, B1 1DD, West Midlands, UK

ARTICLE INFO

Article History:
Received October 1, 2024
Available online December 31, 2024

Research Article

Keywords:
- *Escherichia coli* (*E. coli*)
- Green Fluorescence Protein (GFP)
- Near-infrared (NIR)
- Photodynamic therapy
- Superparamagnetic iron oxide nanoparticles (SPIONs)

ABSTRACT

Our aim is to provide nanostructures combining photodynamic therapy (PDT) and low-dose radiation therapy (RT) to target Escherichia coli (*E. coli*) and Green Fluorescence Protein-E coli bacteria (GFP-*E. coli*). To accomplish this, we synthesized cubic iron oxide nanoparticles conjugated with 2-deoxy-2-[fluorine-19] fluoro-D-glucose (FDG) and loaded them with indocyanine green (ICG) (referred to as ICG@FDG-MNPs). ICG, which has the potential for PDT, was incorporated into ICG@FDG-MNPs to enable effective combined therapy approach targeting *E. coli* bacteria using an LED beam and LINAC-X-ray source treatment. PDT/RT studies demonstrated that when the nanoconjugate was initially stimulated with the LED beam on *E. coli* and Green Fluorescence Protein-*E. coli* bacteria, radiation damage increased, ultimately leading to bacterial death.

1. Introduction

Bacterial infections caused by pathogens are deadly diseases that have a significant impact on human health and mortality. Significant advances have been made in the treatment of bacterial infections over the last few decades. However, the effectiveness of these antimicrobial agents diminishes over time due to the development of resistant bacteria [1]. Antibiotic-resistant pathogens, including Escherichia coli, caused more than 250,000 deaths due to bacterial infection syndrome worldwide in 2019 [2]. Recent estimates suggest that deaths from drug-resistant bacterial infections will continue to increase in the next few decades [2]. The cocktail of magnetic nanoparticles (MNPs) induces robust immune responses against its components [3]. MNPs are utilized in various therapeutic and diagnostic methods. One of these methods is PDT, which gained importance in recent years, particularly in non-oncological antitumor treatment, as it offers a potential alternative with fewer side effects than existing treatments [4]. The basis of this therapy method is to deliver LED light with wavelengths between 400-700 nm to target cells using a photosensitizing (PS) molecule. This approach aims to enhance the drug's efficacy by inducing apoptosis in the target cell through light stimulation [5]. The fact that PDT induces apoptosis of target cells solely with the assistance of free oxygen has allowed this therapy method to be utilized in treatment of both bacterial infections and cancer [6]. Particularly, current applications in the treatment of multidrug-resistant bacterial infections demonstrate the effectiveness of PDT [7, 8].

There are two different reaction pathways involved in the activity of PDT. The first pathway is photosensitizer that reacts with its oxidizing substrate and second pathway is photosensitizer reacts with ground-state triplet oxygen. These pathways cause formation of reactive oxygen radicals [7]. Current studies suggest the use of nanoparticles to enhance the efficiency of photosensitizers, which is the main component of these reactions [9, 10]. This is because photosensitizers are often hydrophobic and require a carrier system for more effective biodistribution [11]. Nanoparticles conjugated with various photosensitizers have shown significant potential in antimicrobial photodynamic therapy [6, 12].

MNPs promise in the diagnosis and treatment of not only cancer but also bacterial infections [13]. They have gained significant attention in the field of antimicrobial therapy due to their unique properties, which distinguish them from conventional nanoparticles. Their ability to be guided by external magnetic fields and their high surface area make them promising candidates for targeted bacterial delivery and enhanced antimicrobial effects. One of the primary advantages of MNPs is their ability to be directed to specific sites using external magnetic fields. This feature allows for precise localization of nanoparticles

*Corresponding author: bakironder@gmail.com

at infection sites, which improves the efficiency of treatment by ensuring that therapeutic agents are concentrated where they are most needed. The use of magnetic fields enables MNPs to accumulate in targeted tissues, reducing off-target effects in healthy areas [14]. Studies have demonstrated that this magnetic targeting can significantly increase the therapeutic potential of nanoparticles by increasing their local concentration in infected areas, thereby improving antimicrobial efficacy [15]. Additionally, the prolonged retention of MNPs at the site of infection increases their interaction time with bacterial cells, potentially enhancing the treatment outcome. Magnetic nanoparticles can exert antimicrobial effects through several mechanisms. Their ability to disrupt bacterial cell membranes and interfere with cellular processes is a key factor in their antimicrobial activity. Furthermore, MNPs can be functionalized with antimicrobial agents, such as antibiotics or peptides, which can be specifically delivered to the infection site under the influence of a magnetic field. This ensures that antimicrobial agents are concentrated in infection, reducing systemic exposure and minimizing side effects [16]. The localized application of these agents also improves their efficiency in combating resistant bacterial strains [17]. Moreover, MNPs can generate reactive oxygen species (ROS) or induce mechanical damage to bacterial cells, which contributes to their bactericidal effect [15, 18]. This multifaceted approach makes MNPs highly effective in combating bacterial infections, particularly those caused by antibiotic-resistant strains. This functionalization capability enhances the specificity of MNPs in targeting bacterial pathogens and enables the development of customized treatments tailored to specific types of infections or antibiotic-resistant bacteria [16, 19]

MNPs exhibit excellent magnetic saturation due to their strong ferromagnetic properties. They are chemically stable and biocompatible. However, magnetic nanoparticles without surface coating tend to aggregate due to their high surface energies [20]. Polymeric materials, such as polyethylene glycol (PEG), have been widely employed for coating superparamagnetic iron oxide nanoparticles (SPIONs). This is because PEG exhibits lower toxicity, high colloidal stability, biocompatibility, and reduced bacterial adhesion on surfaces. Additionally, the coating or modification of MNPs with PEG has improved morphology, properties, and targeting abilities [21]. Due to their low toxicity, magnetic nanoparticles have recently been actively studied for their antibacterial properties. SPIONs can be used as targeting to disease both porphyrin and non- photosensitizers (PSs) using external magnetic field. This approach helps limit the biodistribution of PSs in non-targeted tissue [11, 22]. However, the limited activity of PSs carried by nanoparticles may also be attributed to insufficient light wavelength for cell penetration and low affinity in bacterial cells, which could potentially pave the way for secondary infections [23]. Surface modifications are implemented on nanoparticles to prevent low selectivity, increase bioavailability and biodistribution, and enhance affinity for bacterial cells. Most photosensitizing substances, such as ICG and methylene blue, are produced with a cationic charge to enhance their affinity for bacteria [23].

Fluorodeoxyglucose (FDG), is a glucose analog commonly used in positron emission tomography (PET) imaging for monitoring metabolic activity. FDG is structurally similar to glucose and is taken up by cells through glucose transporters. Once inside the cell, FDG is phosphorylated, but unlike glucose, it is not further metabolized and thus accumulates within the cell. This characteristic allows FDG to accumulate in areas of high metabolic activity, such as cancer cells or infected tissues, making it useful for imaging these areas. The ability of FDG to accumulate in metabolically active cells is crucial for its role in diagnostic imaging and targeted therapies [24]. The mechanism of FDG-coated MNP uptake by bacteria relies on the ability of FDG to be transported into cells via glucose transporters, which are integral membrane proteins responsible for facilitating glucose entry into cells. Because FDG is structurally similar to glucose, it is recognized and transported by these glucose transporters. Once FDG-coated MNPs enter bacterial cells, the magnetic properties of the nanoparticles allow them to be guided to specific areas using an external magnetic field. This external guidance can help increase the accumulation of the nanoparticles at infection sites, potentially enhancing therapeutic efficacy. The accumulation of FDG within bacterial cells occurs because bacteria, particularly in infected or active metabolic states, have an increased demand for glucose, leading to greater FDG uptake.

The uptake of FDG by bacteria is generally specific to metabolically active cells and depends on the presence of glucose transporters. Bacteria with high metabolic activity, such as those found in infected tissues, tend to take up glucose and its analogs like FDG more efficiently. However, this uptake is not entirely specific to one bacterial species; it depends on the presence of functional glucose transporters on the bacterial surface and the metabolic activity of the bacteria.

While FDG is preferentially taken up by bacteria that are metabolically active and have glucose transporters, not all bacterial species exhibit the same level of uptake. Some bacteria may have fewer glucose transporters, or their metabolic activity may not be sufficient to drive significant FDG uptake. Therefore, while FDG-coated MNPs are more efficiently taken up by certain bacterial species, the process is not entirely specific to a single bacterial type. The efficiency of uptake can vary based on the bacteria's metabolic characteristics and their expression of glucose transporters [25, 26]. Recent studies demonstrate that FDG is a powerful agent for monitoring biochemical and physiological processes in *E. coli*. Matsumoto and co-workers investigated FDG's

conversion to fluorescein by the β-galactosidase enzyme in *E. coli*. A novel microfluidic device was used to analyze efflux pump interactions, aiding in the understanding of bacterial resistance mechanisms [27]. In another study, Landon and co-workers investigates the effects of β-defensins on *E. coli*, using fluorescence microscopy to track FDG-related processes like membrane permeability and bacterial growth dynamics under physiological conditions [28]. These studies highlight FDG's role in visualizing and understanding bacterial processes, particularly in *E. coli.*

Green fluorescent proteins (GFPs) have been extensively utilized as spectroscopic and microscopic probes in a wide range of physiological systems. In this study, E. coli bacteria containing GFP were used to investigate the efficacy of fluorescent photons emitted by GFP in photodynamic therapy [29]. The present report describes the investigation of the antimicrobial efficacy of ICG@FDG-MNPs, which have enhanced bioavailability due to various surface and structural modifications, in the combined treatment approach of PDT/RT.

2. Methods

2.1. Chemicals and Equipment

The chemicals used in cubic iron oxide nanoparticle synthesis and tetraethyl orthosilicate (TEOS) were supplied from Merck KGaA (Darmstadt, Germany).

NaF and 2-mercaptoethanol were obtained from Fluka (Germany). PEG, NHS, THF, NH_3 (25%), mannose triflate, kryptofix, K_2CO_3, $NaCNBH_3$, ethylenediamine, DMF, APTES, ICG, CDI, MES, NaCl and oleic acid were purchased from Sigma Aldrich (Germany). *Escherichia coli* (*E. coli*) and green fluorescent protein *Escherichia coli* (GFP-*E. coli*) bacteria were supplied from Ege University Department of Biochemistry in Izmir, Turkey, and LINAC (TrueBeam) irradiation was performed at Medicana Hospital in Izmir, Turkey.

Size and zeta potential measurements of nanoparticles and viability analyses of bacteria were carried out with the following devices located at the Ege University Institute of Nuclear Sciences: Zeta Sizer (Malvern Nano ZS DLS, Malvern, UK), A plate reader (Biotek, Elx800 Universal Absorbance Microplate Reader, USA), a microscope (Leica Microsystems, Germany), a hemocytometer (Carl Zeiss, Jena Germany), an EVOS XL imaging system (Thermofisher, UK).

2.2. Chemicals and Equipment

Synthesis of iron oxide nanoparticles was prepared according to Martinez-Bobueta *et al*. [12]. For the synthesis, 0.353 g (1 mmol) Fe(acac)3 was mixed with 0.688 g (4 mmol) decanoic acid in 25 mL dibenzyl ether. After heating at 60°C (30 min), the solution temperature was increased to 200°C and stirred with a magnetic stirrer under argon flow at 800 rpm for 2h. At the end of 2 hours, the solution temperature was increased to reflux temperature (300oC) and stirred at 800 rpm for 1h. The solution was cooled for 1 h and the nanoparticles were washed 3 times with ethanol using magnets and redispersed in ethanol.

Surface modifications with silica and silane were synthesized by modifying our previous method [30]. C-Fe_3O_4 nanoparticles (100 mg) were dispersed using ultrasonication in a mixture of ethanol and distilled water with a total volume of 10 mL. pH was adjusted to 9 with ammonia (NH_3) solution. 2.5 mL TEOS was added dropwise, and the mixture was heated to 40°C under reflux. The solution was stirred at this temperature at 600 rpm for 12 hours. In the second step, a similar process was used for the synthesis of C-Fe_3O_4@SiO_2-NH_2 nanoparticles. For this, 3 mL of APTES was added to the C-Fe_3O_4@SiO_2 nanoparticles (100 mg) dropwise, and the mixture was stirred under reflux at 600 rpm at 60°C for 14 h. In both steps, the precipitate was separated by magnetization and washed several times with ethanol. Nanoparticles were stored in ethanol at 4°C.

PEGylation was performed following the method described by Zhang's report [31]. Prior to surface modification, the C-Fe_3O_4@SiO_2-NH_2 nanoparticles were dried to remove any adsorbed water. 12 mg of PEG (Poly (ethylene glycol) 2-aminoethyl ether acetic acid) was dissolved in 3 mL of THF. The C-Fe_3O_4@SiO_2-NH_2 nanoparticles, dispersed in THF, were mixed with a 1:1 weight ratio of PEG overnight at 60°C. Then, distilled water was added to the mixture with ultrasonic agitation, and THF was allowed to evaporate overnight.

Synthesis of FDG and conjugation with MNPs were carried out similarly to our previous method [24, 32]. ICG-bound FDG-MNP was synthesized using previously reported methods [24, 33]. FDG-MNP was activated by CDI and then bound to the sulfo groups of ICG through the OH groups on the nanoparticle surface.

2.3. Characterization of Synthesized Nanoparticles

The hydrodynamic diameters were analyzed using Malvern Nano-ZS DLS. The nanoparticles were kept in an ultrasonic bath for 30 minutes and then passed through 0.45 μm filters. Results are expressed as mean ± standard deviation.

SEM and TEM images were taken at Ege University Central Research Laboratory (MATAL) and Eskişehir Osmangazi University Central Research Laboratory Application and Research Center (ARUM). For SEM imaging, FDG-MNP was dried and dissolved in ethanol and coated with 80% Au and 20% Pd. The sample was prepared by drying a carbon-coated copper grid in a dilute ethanol suspension at room temperature. High-resolution TEM images were obtained by dispersing the powder in methanol, stirring with ultrasound for

a few minutes, followed by pipetting one drop onto a carbon support film on a 3 mm copper grid.

2.4. Photodynamic Therapy/Radiotherapy

Four different working groups were formed for PDT and RT experiments of ICG@FDG-MNPs. 1-2 ml of each bacterial sample (sterile saline, PBS, dH_2O) was taken and read at 620 nm to determine the Mc Farland value. An absorbance value of 0.1 corresponds to a Mc Farland turbidity value of 0.5 Mc Farland pattern. *E. coli* (*Escherichia coli*) and GFP-*E. coli* (Green Fluorescent Protein *Escherichia coli*) bacteria were inoculated in Nutrient Broth medium with 0.5 Mc Farland pattern turbidity on 96 well plates, respectively, concentrations of FDG-MNP (1, 2, 10, 20, 100 µg/ µL) (Fig 2) was added in duplicate, and absorbance values were read at 620 nm. After the 24-hour incubation period, the absorbance values at 620 nm in each well were measured again to determine the bacterial proliferation. A graph was then plotted using the differences in absorbance. Photodynamic LED light irradiation with a wavelength of 400-700 nm for 5 minutes at 30 cm. This was followed by the administration of a 1 Gy X-ray dose 30 minutes later for 2 minutes. This was conducted with four different sets of samples, each undergoing various combinations of the two treatment methods [34]. The first group was initially exposed to light, followed by radiation after 24 hours. In the second group, the order of exposure was reversed, with radiation administered first, followed by LED light. The LED beam source used had wavelengths of 400-700 nm and a power of 5.1 Jcm^{-2}. The third group was only exposed to an LED beam, while the fourth group was exposed only to radiation. Bacteria-free medium was used as a negative control and only bacteria in the medium without any other substances (like antibiotics,nanoparticles etc.) were used as positive control and exposed to all photodynamic therapy and radiotherapy conditions in the same manner. Viabilities (%) were calculated by dividing the measured absorbance value by the control value as the percentage value. The absorbance of the negative control was considered zero [35, 36].

2.5. Statistical Analysis

The statistical significance was assessed using the Graph Pad Prism version 5.0 for Windows program via one-way ANOVA and linear regression [37]. A one-way analysis of variance was used to compare differences between the *E. Coli* and GFP-*E. Coli* treated groups. Data was expressed as the mean ± standard deviation and $P < 0.05$ was considered to indicate a statistically significant difference.

3. Results and Discussion

3.1. Characterizations

Fig. 1a and Fig. 1b show SEM and TEM images of FDG-MNPs, respectively. The average hydrodynamic diameters for C-Fe3O4 and C-Fe_3O_4@SiO_2 were measured as 159.0±12.0 nm and 162.6±4.0 nm, respectively (Fig. 1c). The hydrodynamic sizes of C-Fe_3O_4@SiO_2-NH_2-PEG nanoparticles and FDG-MNPs were found to be 256.1±9.0 nm and 314.0±4.0 nm, respectively. The decrease in zeta potential from C-Fe_3O_4 to C-Fe_3O_4@SiO_2 is likely due to the surface charge of the silica molecules present on the surface of the Fe_3O_4 nanoparticles. This surface charge reduces the agglomeration of nanoparticles in aqueous media, enabling the magnetic nanoparticles to retain their colloidal structure. SEM and TEM images revealed that the particle size and shape exhibited a smooth, homogeneous spherical morphology, consistent with the literature [38]. Based on the images, the nanoconjugate exhibited a smooth and round surface (Fig. 1a), and the surface coating did not interfere with the structure of the cubic-shaped iron core (Fig. 1b). The surface coating resulted in an increase in the nanoparticle size which was an expected outcome. These results are consistent with our previous studies [24, 32].

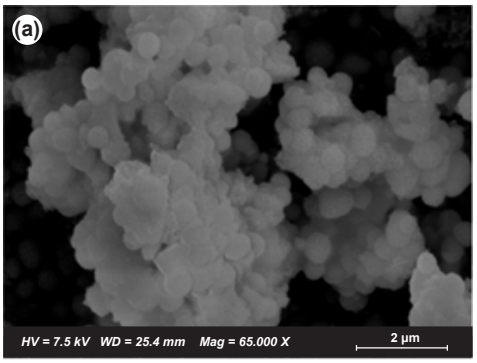

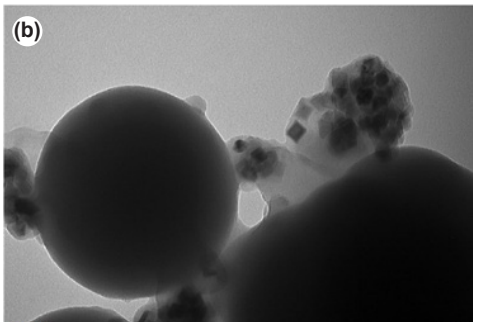

(c)

Nanoconjugates	Hydrodinamic Diameter (d.nm)	Agv. Zeta Potantial (mV)
C-Fe_3O_4	159.0 ± 12.0	+2.51 ± 1.0
C-Fe_3O_4-SiO_2	162.6 ± 4.0	-19.1± 0.6
C-Fe_3O_4-SiO_2-NH_2	163.2 ± 5.0	-36.0± 0.7
C-Fe_3O_4-SiO_2-NH_2PEG	256.1 ± 9.0	-20.4± 1.2
C-Fe_3O_4-SiO_2-NH_2PEG-FDG	314.0 ± 4.0	-24.0± 0.3
C-Fe_3O_4-SiO_2-NH_2PEG-FDG@ICG	120.5 ± 4.5	-16.4± 1.55

Figure 1. (a) SEM image of FDG-MNPs, (b) TEM image of FDG-MNPs and (c) the average hydrodynamic diameters and zeta potential values of nanoparticles.

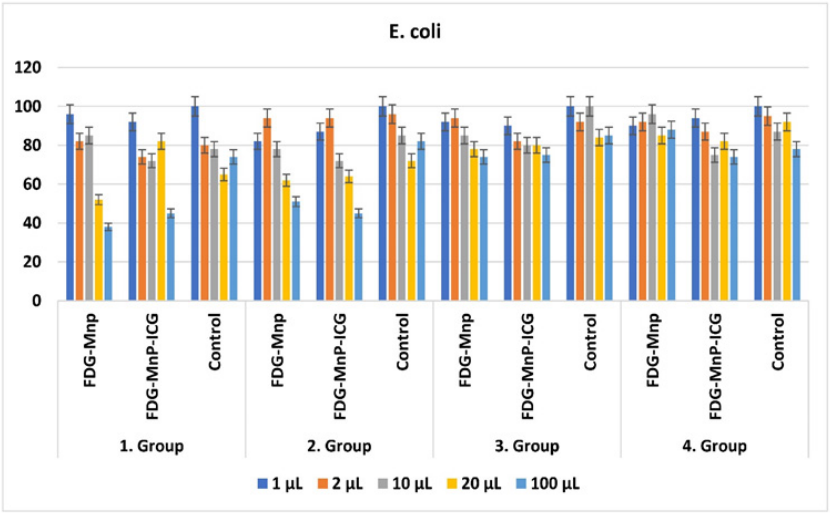

Figure 2. Antimicrobial efficacies of E. Coli in different rates FDG-MNP and ICG@ FDG-MNP concentrations (The 1st group: light first and then radiation, The 2nd group: first radiation and then LED light, The 3rd group: only exposed to an LED beam and 4th group: only exposed to radiation.)

3.2. Photodynamic Therapy/Radiotherapy

Photodynamic therapy has been proven to be effective against biofilm-forming strains and to treat bacteria without resistance to antibiotics [34]. However, its application in deep infections is limited due to the restricted penetration of light [39]. To overcome this limitation, combined treatment methods including photodynamic therapy, are recommended, as current studies have demonstrated their stronger bactericidal effect [40, 41]. In our current study, we observed that the vitality rate for the 1st and 2nd groups, in which light and radiation were applied simultaneously, was lower than the 3rd and 4th groups, where only light or only radiation was applied. Kunz *et al*. demonstrated the effects of PDT on Gram-negative bacteria using LED light at a wavelength of 460 nm using 0.1% riboflavin photosensitizer [42]. Although the vitality rate of *E. coli* bacteria exposed to photodynamic therapy alone (3*rd* group) was higher than that of the groups exposed to combined therapy, the significant decrease in this rate compared to the control group supports the potential use of photodynamic therapy in Gram-negative bacterial biofilms.

In recent years, the use of nanoparticles has become widespread in antibacterial photodynamic therapy and combined therapy methods. Various methods involving nanoparticles have been employed, such as utilizing modified nanoparticles as photosensitizers or as transport systems to enhance the efficient delivery of photosensitizers to bacterial cells [6, 43]. Mohanta *et al*. demonstrated the antibacterial and antibiofilm effect of silver nanoparticles on Gram-negative and multi-drug resistant *E. coli* bacteria microbiota [44].

Aras *et al*. reported that conjugation of ICG with FDG-MNPs provides more accurate and positive results in tumor monitoring [45]. In our study, when evaluating the results, the bactericidal effect of FDG-MNPs and ICG@FDG-MNPs was found to be higher than that of the control groups (see Fig 2 and Fig 3).

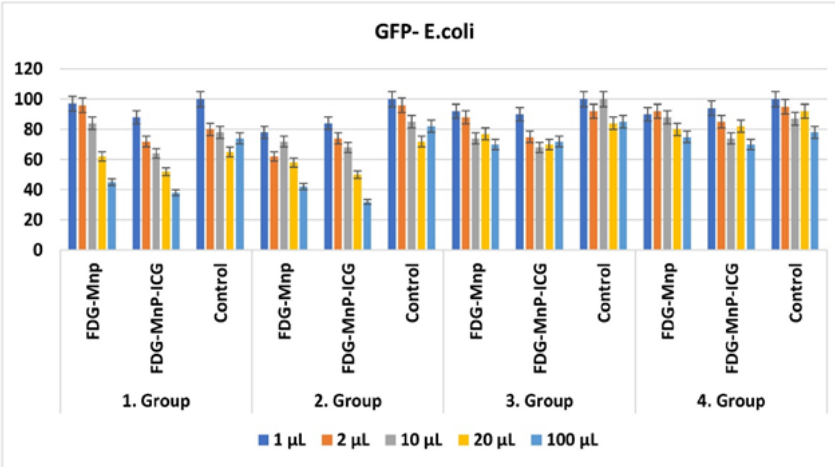

Figure 3. Antimicrobial efficacies of GFP-E.Coli in different rates FDG-MNP and ICG@ FDG-MNP concentrations (The 1st group: light first and then radiation, The 2nd group: first radiation and then LED light, The 3rd group: only exposed to an LED beam and 4th group: only exposed to radiation.)

Combined photodynamic and low-dose radiation therapy for cancer cell damage has been previously reported [34, 35, 46]. Tekin *et al*. reported that PC3 and LNCaP cell viability was significantly reduced when light and radiation were applied using SPHINX-conjugated Pt@TiO nanoparticles. Our study also demonstrated the antibacterial efficacy of the combined treatment method developed and tested for cancer. Radiation creates reactive oxygen species in the living media and causes excitation and ionization. ICG as a light-sensitive dye activates reactive oxygen species (ROS) with radiation in the living media. The effect of light synergistically enhances the radiation damage of ROS [35].

Bacteria-free medium was used as a negative control, and only bacteria in the medium without any antibiotics or nanoparticles etc. were used as a positive control group. In the control group, bacterial damage decreases with increasing concentration. Bilici *et al*. reported that ICG-conjugated SPIONs in photodynamic therapy methods, incorporating PDT and photothermal therapy (PTT), provide an effective and alternative antibacterial therapy even in the absence of antibiotics [47]. Magesan *et al*. reported that the Fe_2O_3-TiO_2 nanocomposites on bacteria have remarkably antibacterial activity against *E. coli* [48]. Photodynamic therapy using nanoparticular systems may be a new solution for the treatment of drug-resistant bacterial infections [48, 49].

The increase in antibiotic resistance in recent years has sparked increased interest in non-antibiotic treatment methods for bacterial infections. Photodynamic therapy (PDI) has received attention in recent years due to its high effectiveness. Furthermore, low-dose X-irradiation shows potential as a more effective treatment when combined with photodynamic therapy. Radiation therapy is commonly used for cancer treatment, but its application in the treatment of bacterial infections, such as caused by *E. coli*, is a developing area of research. The concept of using radiation to kill bacteria or prevent their growth isn't new, and in some cases, ultraviolet (UV) or X-rays have been tested as potential antibacterial agents [50-52]. The use of radiation as a clinical tool for treating infections is still an experimental area and studies are limited in the literature concerning the bacteria and clinical radiotherapy applications. Typically, radiation therapy is generally combined with other agents (such as antibiotics) to increase effectiveness, and its safety and efficacy depend heavily on the dose and type of radiation used, as well as the duration of exposure [53-55]. However, ionizing radiation, such as X-rays and gamma rays, is widely used in clinical settings for local treatment. For instance, in 1982, Luckey proposed that low dose ionizing radiation (LDI) could be beneficial to animal health and survival. This hypothesis has since been supported by several studies, reinforcing the potential positive impacts of LDI on health [56-58] (In our previous studies, we reported that the combined use of different nanoparticles, low-dose X-ray therapy, and photodynamic therapy yields effective results in various cancers [35, 36, 59]. Antibacterial resistance poses a serious threat to human health [38]. The rapid proliferation and mutation of bacteria, along with the overuse of antibiotics and their inappropriate release into the environment, have significantly contributed to the emergence and spread of antibiotic-resistant bacteria. It is crucial to explore innovative therapeutic approaches to overcome antibiotic resistance [5]. Among these approaches, photodynamic therapy (PDT), which is a clinically proven antibacterial therapy, stands out as one of the innovative methods [6]. This approach relies on the interaction of a non-toxic photosensitizer (PS), oxygen, and light of the appropriate wavelength to generate highly reactive oxygen species (ROS). These ROS instantly react with surrounding biomolecules and damage their bioactive components, such as cytoplasmic membranes. In this way, it leads to irreversible cell inactivation, affecting intracellular proteins and DNA [7]. Various compounds such as TiO_2 [8], fullerenes, phenylenes [10], methylene blue [11, 12] and porphyrins [23, 24] have been used for this purpose. However, due to the differences in structure and physicochemical properties of PSs, as well as the variability in bacterial membrane structures, PSs demonstrate activity against specific bacterial species or strains. Therefore, the design and discovery of new PSs that can achieve higher efficiency against a broader range of bacteria remain a significant challenge.

The treatment of bacterial biofilms presents a significant challenge in wounds, primarily due to the limited penetration of antibiotics. Wounds containing biofilms of antibiotic-resistant bacteria have an even poorer prognosis. To enhance biocompatibility and reduce toxicity, we modified our nanoparticles with PEG in a simple one-step reaction. We propose a combined therapy approach that involves low-dose X-ray therapy in conjunction with photodynamic therapy, where the external application of our pegylated FDG-MNP nanoparticles deactivates biofilms and resistance mechanisms [59].

MNPs have other innovative potential applications in (*i*) therapy with hyperthermia [32] and (*ii*) in imaging as magnetic resonance imaging (MRI) probes [60]. Mahandran *et al*. demonstrated the utility of FDG MNPs in magnetic hyperthermia and cancer therapy. Magnetic hyperthermia is based on the local application of a magnetic field, causing damage to the tumor by increasing its temperature above body temperature [32]. Photodynamic therapy combined with low-dose radiotherapy that damages cancer or bacterial cells via reactive oxygen species (ROS) may be more effective in common bacterial infections resistant to antibiotics.

The nanoparticles exhibit lower oxidation and relatively low toxicity in comparison to many other materials, such as iron, nickel, and cobalt. Moreover, new bioconjugates can be developed to enhance their bioavailability, such as the use of FDG labeled with

nonradioactive ^{19}F, as a conjugate to increase their affinity for both cancer cells [61, 62] and infections [63]. This research can establish the safety of its *in vivo* applications and explore its potential in cancer treatment, while also unlocking possibilities for other medical applications. The obtained results would offer valuable guidance for the future development of multifunctional agents and the further optimization of their diagnostic performance in clinical settings.

4. Conclusions

In conclusion, we have observed that the ICG@FDG-MNP exhibits greater efficacy, particularly against GFP-*E. coli* bacterial strains. Furthermore, the combined therapy approach proves to be more effective in terms of its antibacterial effects compared to radiotherapy or photodynamic therapy alone. In future studies, we recommend conducting more comprehensive investigations into the antibacterial effects of photosensitizers and further defining the effectiveness of combined treatment methods for infectious diseases.

5. Acknowledgements

Authors thank Prof Dr Serap Evran from Ege University, Department of Biochemistry in Izmir-Turkey for the green fluorescent bacteria she gifted and Dr. Funda Manalp and Alpman Manalp for LINAC irradiation in Medicana Hospital, Izmir/Turkey. The work was partially presented at the International Nuclear Sciences and Technologies Conference (INSTEC-22).

6. Conflicts of Interest

The authors declare no conflict of interest.

Abbreviations	Descriptions
C-Fe_3O_4	Cubic iron oxide
C-Fe_3O_4-SiO_2	Cubic iron oxide coated with TEOS
C-Fe_3O_4-SiO_2-NH_2	Cubic iron oxide coated with TEOS and APTES
C-Fe_3O_4-SiO_2-NH_2-PEG	Cubic iron oxide coated with TEOS, APTES and PEG
FDG	2-deoxy-2-[fluorine19]fluoro-D-glucose
FDG-MNPs	Silica and silane coated, PEGylated and FDG conjugated iron oxide magnetic nanoparticles
ICG	Indocyanine green
ICG@FDG-MNPs	ICG loaded FDG conjugated magnetic iron oxide nanoparticles
NPs	Nanoparticles
SPIONs	Superparamagnetic iron oxide nanoparticles
MNPs	Magnetic iron oxide nanoparticles

References

[1] S. K. Singh *et al.*, "Review of Photoresponsive Plasmonic Nanoparticles That Produce Reactive Chemical Species for Photodynamic Therapy of Cancer and Bacterial Infections", *ACS Appl Nano Mater*, vol. 6, no. 3, pp. 1508-1521, Feb. 2023, doi: 10.1021/acsanm.2c04551.

[2] G. Li, Z. Lai, and A. Shan, "Advances of Antimicrobial Peptide-Based Biomaterials for the Treatment of Bacterial Infections", *Advanced Science*, vol. 10, no. 11, p. 2206602, Apr. 2023, doi: https://doi.org/10.1002/advs.202206602.

[3] M. Abkar, S. Alamian, and N. Sattarahmady, "Gelatin Micro/Nanoparticles-Based Delivery of Urease and Omp31 in Mice Has a Protective Role Against Brucella melitensis 16 M Infection", *Bionanoscience*, vol. 13, pp. 1-9, Feb. 2023, doi: 10.1007/s12668-023-01073-6.

[4] U. Chilakamarthi and L. Giribabu, "Photodynamic Therapy: Past, Present and Future", *The Chemical Record*, vol. 17, no. 8, pp. 775-802, Aug. 2017, doi: https://doi.org/10.1002/tcr.201600121.

[5] Q. Zhang and L. Li, "Photodynamic combinational therapy in cancer treatment", *J BUON*, vol. 23, no. 3, pp. 561-567, 2018, [Online]. Available: http://europepmc.org/abstract/MED/30003719

[6] S. Perni, P. Prokopovich, J. Pratten, I. P. Parkin, and M. Wilson, "Nanoparticles: their potential use in antibacterial photodynamic therapy", *Photochemical & Photobiological Sciences*, vol. 10, no. 5, pp. 712-720, 2011, doi: 10.1039/C0PP00360C.

[7] S. Kwiatkowski *et al.*, "Photodynamic therapy-mechanisms, photosensitizers and combinations", *Biomedicine & Pharmacotherapy*, vol. 106, pp. 1098-1107, 2018, doi: https://doi.org/10.1016/j.biopha.2018.07.049.

[8] X. Wang *et al.*, "Analysis of the In Vivo and In Vitro Effects of Photodynamic Therapy on Breast Cancer by Using a Sensitizer, Sinoporphyrin Sodium", *Theranostics*, vol. 5, no. 7, pp. 772-786, 2015, doi: 10.7150/thno.10853.

[9] X. Dai, X. Li, Y. Liu, and F. Yan, "Recent advances in nanoparticles-based photothermal therapy synergizing with immune checkpoint blockade therapy", *Mater Des*, vol. 217, p. 110656, 2022, doi: https://doi.org/10.1016/j.matdes.2022.110656.

[10] D. Wang *et al.*, "Targeted Iron-Oxide Nanoparticle for Photodynamic Therapy and Imaging of Head and Neck Cancer", *ACS Nano*, vol. 8, no. 7, pp. 6620-6632, Jul. 2014, doi: 10.1021/nn501652j.

[11] M. Saeed, W. Ren, and A. Wu, "Therapeutic applications of iron oxide based nanoparticles in cancer: basic concepts and recent advances", *Biomater Sci*, vol. 6, no. 4, pp. 708-725, 2018, doi: 10.1039/C7BM00999B.

[12] C. Martinez-Boubeta *et al.*, "Learning from Nature to Improve the Heat Generation of Iron-Oxide Nanoparticles for Magnetic Hyperthermia Applications", *Sci Rep*, vol. 3, no. 1, p. 1652, 2013, doi: 10.1038/srep01652.

[13] B. Anegbe, I. H. Ifijen, M. Maliki, I. E. Uwidia, and A. I. Aigbodion, “Graphene oxide synthesis and applications in emerging contaminant removal: a comprehensive review”, *Environ Sci Eur*, vol. 36, no. 1, p. 15, 2024, doi: 10.1186/s12302-023-00814-4.

[14] K. Bin Liew *et al.*, “A review and revisit of nanoparticles for antimicrobial drug delivery”, *J Med Life*, vol. 15, pp. 328-335, Apr. 2022, doi: 10.25122/jml-2021-0097.

[15] J. Chomoucka, J. Drbohlavova, D. Huska, V. Adam, R. Kizek, and J. Hubalek, “Magnetic nanoparticles and targeted drug delivering”, *Pharmacol Res*, vol. 62, no. 2, pp. 144-149, 2010, doi: https://doi.org/10.1016/j.phrs.2010.01.014.

[16] E. Kianfar, “Magnetic Nanoparticles in Targeted Drug Delivery: a Review”, *J Supercond Nov Magn*, Jun. 2021, doi: 10.1007/s10948-021-05932-9.

[17] Q A Pankhurst, J Connolly, S K Jones, and J Dobson, “Applications of magnetic nanoparticles in biomedicine”, *J Phys D Appl Phys*, vol. 36, no. 13, p. R167, 2003, doi: 10.1088/0022-3727/36/13/201.

[18] Z. Yu *et al.*, “Reactive Oxygen Species-Related Nanoparticle Toxicity in the Biomedical Field”, *Nanoscale Res Lett*, vol. 15, no. 1, p. 115, 2020, doi: 10.1186/s11671-020-03344-7.

[19] P. Farinha, J. Coelho, C. Reis, and M. Gaspar, “A Comprehensive Updated Review on Magnetic Nanoparticles in Diagnostics”, *Nanomaterials*, vol. 11, p. 3432, Dec. 2021, doi: 10.3390/nano11123432.

[20] V. I. Shubayev, T. R. Pisanic, and S. Jin, “Magnetic nanoparticles for theragnostics”, *Adv Drug Deliv Rev*, vol. 61, no. 6, pp. 467-477, 2009, doi: https://doi.org/10.1016/j.addr.2009.03.007.

[21] E. Illés, E. Tombácz, M. Szekeres, I. Y. Tóth, Á. Szabó, and B. Iván, “Novel carboxylated PEG-coating on magnetite nanoparticles designed for biomedical applications”, *J Magn Magn Mater*, vol. 380, pp. 132-139, 2015, doi: https://doi.org/10.1016/j.jmmm.2014.10.146.

[22] O. J. Fakayode, N. Tsolekile, S. P. Songca, and O. S. Oluwafemi, “Applications of functionalized nanomaterials in photodynamic therapy”, *Biophys Rev*, vol. 10, no. 1, pp. 49-67, 2018, doi: 10.1007/s12551-017-0383-2.

[23] B. A. Thomas-Moore, C. A. del Valle, R. A. Field, and M. J. Marín, “Recent advances in nanoparticle-based targeting tactics for antibacterial photodynamic therapy”, *Photochemical & Photobiological Sciences*, vol. 21, no. 6, pp. 1111-1131, 2022, doi: 10.1007/s43630-022-00194-3.

[24] V. Yasakci, V. Tekin, O. Kozgus, V. Evren, and P. Unak, “Hyaluronic acid-modified [19F]FDG-conjugated magnetite nanoparticles: in vitro bioaffinities and HPLC analyses in organs”, *J Radioanal Nucl Chem*, vol. 318, Oct. 2018, doi: 10.1007/s10967-018-6282-6.

[25] M. Hu, G. Chen, L. Luo, and L. Shang, “A Systematic Review and Meta-Analysis on the Accuracy of Fluorodeoxyglucose Positron Emission Tomography/Computerized Tomography for Diagnosing Periprosthetic Joint Infections”, *Front Surg*, vol. 9, 2022, [Online]. Available: https://www.frontiersin.org/journals/surgery/articles/10.3389/fsurg.2022.698781

[26] Y. Yao *et al.*, “Nanoparticle-Based Drug Delivery in Cancer Therapy and Its Role in Overcoming Drug Resistance”, *Front Mol Biosci*, vol. 7, 2020, [Online]. Available: https://www.frontiersin.org/journals/molecular-biosciences/articles/10.3389/fmolb.2020.00193

[27] Y. Matsumoto *et al.*, “Evaluation of Multidrug Efflux Pump Inhibitors by a New Method Using Microfluidic Channels”, *PLoS One*, vol. 6, p. e18547, Apr. 2011, doi: 10.1371/journal.pone.0018547.

[28] C. Landon *et al.*, “Real-Time Fluorescence Microscopy on Living E. coli Sheds New Light on the Antibacterial Effects of the King Penguin β-Defensin AvBD103b”, *Int J Mol Sci*, vol. 23, no. 4, 2022, doi: 10.3390/ijms23042057.

[29] S. K. Gogoi, P. Gopinath, A. Paul, A. Ramesh, S. S. Ghosh, and A. Chattopadhyay, “Green Fluorescent Protein-Expressing Escherichia coli as a Model System for Investigating the Antimicrobial Activities of Silver Nanoparticles”, *Langmuir,* vol. 22, no. 22, pp. 9322-9328, Oct. 2006, doi: 10.1021/la060661v.

[30] E. Tutun, V. Tekin, V. Yasakcı, Ö. Aras, and P. Ünak, “Synthesis and morphological studies of Tc-99m-labeled lupulone-conjugated Fe3O4@TiO2 nanocomposite, and in vitro cytotoxicity activity on prostate cancer cell lines”, *Appl Organomet Chem*, vol. 35, no. 12, p. e6435, Dec. 2021, doi: https://doi.org/10.1002/aoc.6435.

[31] Y. Zhang, N. Kohler, and M. Zhang, “Surface modification of superparamagnetic magnetite nanoparticles and their intracellular uptake”, *Biomaterials*, vol. 23, no. 7, pp. 1553-1561, 2002, doi: https://doi.org/10.1016/S0142-9612(01)00267-8.

[32] M. Subramanian *et al.*, “A Pilot Study Into the Use of FDG-mNP as an Alternative Approach in Neuroblastoma Cell Hyperthermia”, *IEEE Trans Nanobioscience*, vol. 15, p. 1, Jul. 2016, doi: 10.1109/TNB.2016.2584543.

[33] K. L. Carraway and R. B. Triplett, “Reaction of carbodiimides with protein sulfhydryl groups”, *Biochimica et Biophysica Acta (BBA)-Protein Structure*, vol. 200, no. 3, pp. 564-566, 1970, doi: https://doi.org/10.1016/0005-2795(70)90112-1.

[34] C. Ozada, V. Tekin, F. B. Barlas, S. Timur, and P. Unak, “Protoporphyrin-IX and Manganese Oxide Nanoparticles Encapsulated in Niosomes as Theranostic”, *ChemistrySelect,* vol. 5, no. 6, pp. 1987-1993, Feb. 2020, doi: https://doi.org/10.1002/slct.201901620.

[35] V. Tekin *et al.*, “A novel anti-angiogenic radio/photo sensitizer for prostate cancer imaging and therapy: 89Zr-Pt@TiO2-SPHINX, synthesis and in vitro evaluation”, *Nucl Med Biol*, vol. 94-95, pp. 20-31, 2021, doi: https://doi.org/10.1016/j.nucmedbio.2020.12.005.

[36] B. Demir, F. B. Barlas, Z. P. Gumus, P. Unak, and S. Timur, “Theranostic Niosomes as a Promising Tool for Combined Therapy and Diagnosis: ‘All-in-One’ Approach”, *ACS Appl Nano Mater*, vol. 1, no. 6, pp. 2827-2835, Jun. 2018, doi: 10.1021/acsanm.8b00468.

[37] P. Kumar, A. V Ranawade, and N. G. Kumar, “Potential

Probiotic Escherichia coli 16 Harboring the Vitreoscilla Hemoglobin Gene Improves Gastrointestinal Tract Colonization and Ameliorates Carbon Tetrachloride Induced Hepatotoxicity in Rats", *Biomed Res Int*, vol. 2014, no. 1, p. 213574, Jan. 2014, doi: https://doi.org/10.1155/2014/213574.

[38] S. Moritake *et al.*, "Functionalized Nano-Magnetic Particles for an In Vivo Delivery System", *Journal Nanosci Nanotechnol*, vol. 7, pp. 937-944, apr. 2007, doi: 10.1166/jnn.2007.216.

[39] Y. Wang *et al.*, "Enhanced antimicrobial activity through the combination of antimicrobial photodynamic therapy and low-frequency ultrasonic irradiation", *Adv Drug Deliv Rev*, vol. 183, p. 114168, 2022, doi: https://doi.org/10.1016/j.addr.2022.114168.

[40] M. Ribeiro, I. B. Gomes, M. J. Saavedra, and M. Simões, "Photodynamic therapy and combinatory treatments for the control of biofilm-associated infections", *Lett Appl Microbiol*, vol. 75, no. 3, pp. 548-564, Sep. 2022, doi: https://doi.org/10.1111/lam.13762.

[41] R. Youf *et al.*, "Antimicrobial Photodynamic Therapy: Latest Developments with a Focus on Combinatory Strategies", *Pharmaceutics*, vol. 13, no. 12, 2021, doi: 10.3390/pharmaceutics13121995.

[42] D. Kunz, J. Wirth, A. Sculean, and S. Eick, "In-vitro-activity of additive application of hydrogen peroxide in antimicrobial photodynamic therapy using LED in the blue spectrum against bacteria and biofilm associated with periodontal disease", *Photodiagnosis Photodyn Ther,* vol. 26, pp. 306-312, 2019, doi: https://doi.org/10.1016/j.pdpdt.2019.04.015.

[43] V. Secchi, A. Monguzzi, and I. Villa, "Design Principles of Hybrid Nanomaterials for Radiotherapy Enhanced by Photodynamic Therapy", *Int J Mol Sci*, vol. 23, p. 8736, Aug. 2022, doi: 10.3390/ijms23158736.

[44] Y. K. Mohanta, K. Biswas, S. K. Jena, A. Hashem, E. F. Abd_Allah, and T. K. Mohanta, "Anti-biofilm and Antibacterial Activities of Silver Nanoparticles Synthesized by the Reducing Activity of Phytoconstituents Present in the Indian Medicinal Plants", *Front Microbiol*, vol. 11, 2020, [Online]. Available: https://www.frontiersin.org/journals/microbiology/articles/10.3389/fmicb.2020.01143

[45] O. Aras *et al.*, "An in-vivo pilot study into the effects of FDG-mNP in cancer in mice", *PLoS One*, vol. 13, p. e0202482, Aug. 2018, doi: 10.1371/journal.pone.0202482.

[46] F. Barlas *et al.*, "Multimodal Theranostic Assemblings: Double Encapsulation of Protoporphyrine-IX/Gd3+ in Niosomes", *RSC Adv*, vol. 6, Mar. 2016, doi: 10.1039/C5RA26737D.

[47] K. Bilici *et al.*, "Broad spectrum antibacterial photodynamic and photothermal therapy achieved with indocyanine green loaded SPIONs under near infrared irradiation", *Biomater Sci*, vol. 8, no. 16, pp. 4616-4625, 2020, doi: 10.1039/D0BM00821D.

[48] P. Magesan *et al.*, "Photodynamic and antibacterial studies of template-assisted Fe2O3-TiO2 nanocomposites", *Photodiagnosis Photodyn Ther*, vol. 40, p. 103064, 2022, doi: 10.1016/j.pdpdt.2022.103064.

[49] X. Cui *et al.*, "Charge adaptive phytochemical-based nanoparticles for eradication of methicillin-resistant staphylococcus aureus biofilms", *Asian J Pharm Sci*, vol. 19, no. 3, p. 100923, 2024, doi: https://doi.org/10.1016/j.ajps.2024.100923.

[50] S. F. Alanazi, "Evaluating the effect of X ray irradiation in the control of food bacterial pathogens", *J King Saud Univ Sci*, vol. 35, no. 1, p. 102367, 2023, doi: https://doi.org/10.1016/j.jksus.2022.102367.

[51] J. Cherif, A. Raddaoui, M. Trabelsi, and N. Souissi, "Diagnostic low-dose X-ray radiation induces fluoroquinolone resistance in pathogenic bacteria", *Int J Radiat Biol,* vol. 99, no. 12, pp. 1971-1977, Dec. 2023, doi: 10.1080/09553002.2023.2232016.

[52] V. Yemmireddy, A. Adhikari, and J. Moreira, "Effect of ultraviolet light treatment on microbiological safety and quality of fresh produce: An overview", *Front Nutr*, vol. 9, 2022, [Online]. Available: https://www.frontiersin.org/journals/nutrition/articles/10.3389/fnut.2022.871243

[53] O. Langer *et al.*, "Synthesis of fluorine-18-labeled ciprofloxacin for PET studies in humans", *Nucl Med Biol*, vol. 30, no. 3, pp. 285-291, 2003, doi: https://doi.org/10.1016/S0969-8051(02)00444-4.

[54] M. Silindir-Gunay and A. Y. Ozer, "99mTc-radiolabeled Levofloxacin and micelles as infection and inflammation imaging agents", *J Drug Deliv Sci Technol*, vol. 56, p. 101571, 2020, doi: https://doi.org/10.1016/j.jddst.2020.101571.

[55] A. Signore *et al.*, "Imaging Bacteria with Radiolabelled Probes: Is It Feasible?", *J Clin Med*, vol. 9, no. 8, 2020, doi: 10.3390/jcm9082372.

[56] J. Li *et al.*, "Effects of low-dose X-ray irradiation on activated macrophages and their possible signal pathways", *PLoS One*, vol. 12, p. e0185854, Oct. 2017, doi: 10.1371/journal.pone.0185854.

[57] A. Liebmann *et al.*, "Low-Dose X-Irradiation ofAdjuvant-Induced Arthritis in Rats", *Strahlentherapie und Onkologie*, vol. 180, no. 3, pp. 165-172, 2004, doi: 10.1007/s00066-004-1197-2.

[58] T. D. Luckey, "Physiological Benefits from Low Levels of Ionizing Radiation", *Health Phys*, vol. 43, no. 6, 1982, [Online]. Available: https://journals.lww.com/health-physics/fulltext/1982/12000/physiological_benefits_from_low_levels_of_ionizing.1.aspx.

[59] A. K. Lam *et al.*, "PEGylation of Polyethylenimine Lowers Acute Toxicity while Retaining Anti-Biofilm and β-Lactam Potentiation Properties against Antibiotic-Resistant Pathogens", *ACS Omega*, vol. 5, no. 40, pp. 26262-26270, Oct. 2020, doi: 10.1021/acsomega.0c04111.

[60] M. Bravo *et al.*, "Nanoparticle-mediated thermal Cancer therapies: Strategies to improve clinical translatability", *Journal of Controlled Release*, vol. 372, pp. 751-777, 2024, doi: https://doi.org/10.1016/j.jconrel.2024.06.055.

[61] J. M. Gillies, C. Prenant, G. N. Chimon, G. J. Smethurst, B. A. Dekker, and J. Zweit, "Microfluidic technology for PET radiochemistry", *Applied Radiation and Isotopes*, vol. 64, no. 3, pp. 333-336, 2006, doi: https://doi.org/10.1016/j.apradiso.2005.08.009.

[62] G. Unak *et al.*, “Gold nanoparticle probes: Design and in vitro applications in cancer cell culture”, *Colloids Surf B Biointerfaces*, vol. 90, pp. 217-226, 2012, doi: https://doi.org/10.1016/j.colsurfb.2011.10.027.

[63] L. M. V. Knappe Frederik Anton; Giovanella Luca; Luster Markus; Librizzi Damiano, “Diagnostic value of FDG-PET/CT in the diagnostic work-up of inflammation of unknown origin”, *Nuklearmedizin-NuclearMedicine*, vol. 62, no. 01, pp. 27-33, 2023, doi: 10.1055/a-1976-1765.